Proceedings of the XVIII ECSMGE 2024
GEOTECHNICAL ENGINEERING CHALLENGES
TO MEET CURRENT AND EMERGING NEEDS OF SOCIETY
© 2024 the Authors
ISBN 978-1-032-54816-6
DOI 10.1201/9781003431749-319
Open Access: www.taylorfrancis.com, CC BY-NC-ND 4.0 license

ECSMGE 24
XVIII EUROPEAN CONFERENCE ON SOIL MECHANICS AND GEOTECHNICAL ENGINEERING

Finite element modelling of a tailings dam using the Clay and Sand Model

Modélisation par éléments finis des barrages de retenue de résidus miniers à l'aide du Clay And Sand Model

A. Laera*
Seequent, the Bentley Subsurface Company, Milan, Italy

V.H. Miranda
Civil Engineering & Geo-Sciences, Delft University of Technology, Delft, The Netherlands

R.J N. Azeiteiro
Seequent, the Bentley Subsurface Company, London, United Kingdom

T. Bui, S. Brasile
Seequent, the Bentley Subsurface Company, Delft, The Netherlands

R.B.J. Brinkgreve
Civil Engineering & Geo-Sciences, Delft University of Technology, Delft, The Netherlands

**anita.laera@seequent.com*

ABSTRACT: Tailings dam failures are one of the most destructive phenomena, both in terms of number of victims and of generated environmental impact. Over the years, different causes have been identified, with flow liquefaction being a prominent factor to consider when assessing the stability of tailings deposits. Due to the complexity of these events, numerical models are crucial for the analysis and design phases, where appropriate advanced soil constitutive models must be selected to reproduce the relevant features of the soil behaviour. In this paper, the Clay And Sand Model (CASM), originally proposed by Yu (1998) and later modified by Arroyo and Gens (2021) and Manica et al. (2021), has been adopted for the simulation of flow liquefaction of tailings deposits. The model incorporates the state parameter concept (Been and Jefferies, 1985) and has been implemented as a User-Defined Soil Model (UDSM) into the finite element code PLAXIS; thereby, it becomes generally applicable to a wide range of geotechnical applications. Due to its versatile yield surface and plastic potential formulations, CASM can be used to model the behaviour of a wide range of soils, from fine-grained (e.g., clays) to coarser-grained soils (e.g., silts and sands). This paper shows the capability of the model, as well as the robustness of the finite element formulation, to reproduce the soil flow liquefaction observed in boundary value problems.

RÉSUMÉ: Les ruptures de barrages de résidus miniers sont l'un des phénomènes les plus destructeurs, tant en termes de nombre de victimes que d'impact environnemental généré. De différentes causes ont été identifiées, parmi eux la liquéfaction statique étant un facteur important pour l'évaluation de la stabilité des dépôts de résidus miniers. En raison de la complexité de ces événements, les modèles numériques sont cruciaux pour les phases d'analyse et de dimensionnement, où des modèles constitutifs avancés doivent être utilisés pour reproduire les caractéristiques pertinentes du comportement du sol. Dans cet article, le Clay And Sand Model (CASM), proposé originalement par Yu (1998) et modifié par Arroyo et Gens (2021) et Manica et al. (2021), a été adopté pour la simulation de la liquéfaction statique des résidus miniers. Le modèle intègre le concept de paramètre d'état (Been et Jefferies, 1985) et a été implémenté en tant que User-Defined Soil Model (UDSM) dans le code des éléments finis PLAXIS; de ce fait, il devient généralement applicable à un grand nombre d'applications géotechniques. Grâce à la flexibilité de la formulation de la surface de charge et du potentiel plastique, CASM peut être utilisé pour modéliser le comportement de plusieurs types de sols, des sols à grain fin (comme les argiles) aux sols à grain plus grossier (comme les limons et les sables). Cet article montre la capacité du modèle, ainsi que la robustesse de la formulation par éléments finis, à reproduire la liquéfaction statique du sol observée dans les structures géotechniques.

Keywords: CASM; flow liquefaction; static liquefaction; tailings dams.

1 INTRODUCTION

Over the last 50 years, several failures of tailings facilities have been recorded around the world, resulting in hundreds of fatalities, and damage to infrastructures and environment. Static (or flow) liquefaction has often been identified as either the main cause of failure, as in the case of the Fundão tailings dam (Morgenstern et al., 2016), or as the major contributor to the devastating consequences of failure, as in the case of the Aznalcóllar dam (Alonso and Gens, 2006). The mechanism underlying flow liquefaction is undrained softening, which occurs when the soil undrained strength reduces significantly after a peak (instability point). This phenomenon is observed in tailings and, more in general, in hydraulic fills that are deposited in a loose state, and may be caused by different triggering mechanisms, such as undrained loading, drained lateral stress reduction, or a change in the hydraulic conditions.

To back-analyse known failure events, evaluate the status of existing tailings dams, or design new tailings facilities, advanced numerical analysis accounting for large deformations, soil non-linearity and softening should be performed. A key element in the numerical simulation of flow liquefaction is the choice of the constitutive model. The Clay And Sand Model (CASM) has been developed by Yu (1998) in the framework of Critical State Soil Mechanics (Schofield and Wroth, 1968) as a versatile constitutive model able to simulate the behaviour of both clays and sands. CASM can simulate static liquefaction and has been successfully employed to analyse the Brumadinho (Arroyo and Gens, 2021) and Merriespruit dam failures (Mánica et al., 2022).

CASM has been implemented as a User-Defined Soil Model (UDSM) in PLAXIS (Bentley Systems Inc, 2023). Compared to the original formulation, this version of CASM includes Lode's angle dependency, an alternative plastic potential equation (Arroyo and Gens, 2021) and the possibility to use it as either a rate-independent plastic model or as an elasto-viscoplastic model accounting for time-dependency (Manica et al., 2021).

In this paper, the Tar Island Dyke failure (Plewes et al., 1989) has been chosen as a case study to be modelled using the rate independent CASM model. After describing the constitutive equations, the finite element model is presented together with the strategy adopted to calibrate the model parameters and the results of the numerical analysis.

2 CONSTITUTIVE EQUATIONS

In the following, soil mechanics convention is used, i.e. stresses are positive in compression. Vectorial and tensorial quantities are denoted in bold, while scalars are in normal character.

2.1 Main concepts

As in the classical elasto-plasticity theory, the total strain rate is decomposed into an elastic $\dot{\boldsymbol{\varepsilon}}^{\boldsymbol{e}}$, and a plastic part $\dot{\boldsymbol{\varepsilon}}^{\boldsymbol{p}}$:

$$\dot{\boldsymbol{\varepsilon}} = \dot{\boldsymbol{\varepsilon}}^{\boldsymbol{e}} + \dot{\boldsymbol{\varepsilon}}^{\boldsymbol{p}} \tag{1}$$

Both strain rate tensors consist of a volumetric part $\dot{\varepsilon}_v$, and a deviatoric part $\dot{\boldsymbol{e}}$:

$$\dot{\boldsymbol{\varepsilon}} = \frac{1}{3}\dot{\varepsilon}_v\boldsymbol{\delta} + \dot{\boldsymbol{e}} \tag{2}$$

where $\boldsymbol{\delta}$ is the second-order identity tensor.

Similarly, the effective stress tensor $\boldsymbol{\sigma'}$ can be decomposed into a hydrostatic part p', and a deviatoric part $\boldsymbol{s}$:

$$\boldsymbol{\sigma'} = \frac{1}{3}p'\boldsymbol{\delta} + \boldsymbol{s} \tag{3}$$

The model has been derived from a reformulation of the original Cam-Clay model in terms of the state parameter ξ, defined as the difference between the specific volume υ at the current state and the specific volume on the critical state line at the same mean pressure p'. A positive value of the state parameter indicates a loose material that, under shearing, shows a volume contraction in drained conditions or an increase in pore pressure and a reduction of p', leading to flow liquefaction, in undrained conditions. The distance between the critical state line (CSL) and the reference consolidation line corresponds to the reference state parameter ξ_R.

2.2 Model formulation

CASM adopts a general stress-state relation to describe the yield surface for a variety of soils:

$$f = \left(\frac{q}{M_\theta p'}\right)^n + \frac{\xi}{\xi_R} - 1 \tag{4}$$

where q is the deviatoric stress, n is a parameter that controls the shape of the yield function, and M_θ is the stress ratio at critical state, dependent on Lode's angle θ according to (Sheng et al., 2000):

$$M_\theta = M\left(\frac{2\alpha^4}{1+\alpha^4+(1-\alpha^4)\sin 3\theta}\right)^{1/4} \quad (5)$$

In Equation 5, M is the critical stress ratio in triaxial compression and α is a parameter controlling the shape of the yield function in the deviatoric plane, both depending on the friction angle φ:

$$M = \frac{6\sin\varphi}{3-\sin\varphi}; \qquad \alpha = \frac{3-\sin\varphi}{3+\sin\varphi} \quad (6)$$

Finally, $\sin 3\theta$ is equal to:

$$\sin 3\theta = -\left(\frac{3\sqrt{3}}{2}\frac{J_3}{J_2^{3/2}}\right) \quad (7)$$

where J_2 and J_3 are the second and third invariant of the deviatoric stress tensor $\boldsymbol{s}$, respectively.

In the model implementation, it is preferred to use an alternative equivalent equation for the yield surface:

$$f = \left(\frac{q}{M_\theta p'}\right)^n + \frac{1}{\ln r}\ln\frac{p'}{p'_0} \quad (8)$$

where r is the spacing ratio and p'_0 is the preconsolidation pressure (Figure 1).

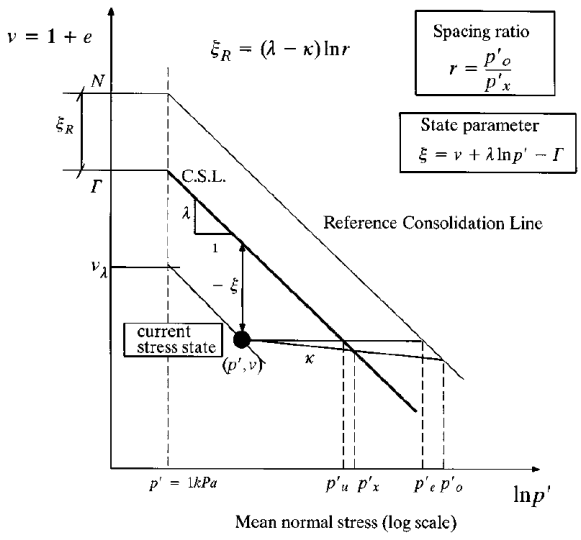

Figure 1. Definitions of state parameter, critical state constants, and reference state parameter (Yu, 1998).

Inside the yield surface, the behaviour is elastic and isotropic, defined by the bulk stiffness K', and the shear stiffness G. K' depends linearly on the mean effective pressure p', while G is a function of the bulk modulus and the coefficient of Poisson ν' (constant):

$$K' = \frac{p'(1+e_0)}{\kappa}; \qquad G = \frac{3(1-2\nu')}{2(1+\nu')}K' \quad (9)$$

where e_0 is the initial void ratio and κ is the slope of the swelling line in the ($\ln p'$, υ) space.

Instead, the plastic strains are calculated based on a non-associated flow rule. The plastic potential g can be described by either the original equation derived from Rowe's stress-dilatancy relationship (Rowe, 1962), or by the one introduced by Arroyo and Gens (2021), overcoming the limitations of the first one for stress paths with low stress ratios. The latter (Eq. 10) has been adopted in this paper:

$$g = \left(\frac{q}{M_\theta p'}\right)^m + m - \frac{p'_c(m-1)}{p'} - 1 \quad (10)$$

where m is a parameter controlling the shape of the plastic potential and p'_c must be solved for the current stress state such that the plastic potential passes through it.

Finally, the same isotropic volumetric hardening rule as in the Cam-Clay models is adopted:

$$\dot{p}'_0 = \frac{\upsilon\,\dot{\varepsilon}_v^p}{\lambda-\kappa}p'_0 \quad (11)$$

where λ is the slope of the CSL and reference line in the ($\ln p'$, υ) space, and $\dot{\varepsilon}_v^p$ is the plastic volumetric strain increment.

3 FINITE ELEMENT MODELLING OF THE TAR ISLAND DYKE

The Tar Island Dyke is a tailings structure built to retain sand tailings for the Suncor oil sand mine in Canada. Plewes et al. (1989) describe that, after an initial construction phase with the centreline method, the upstream construction method with compacted sand has been used for the subsequent phases. Adjacent to it, sand beaches were formed by discharging tailings from the upstream dyke crest.

Failure events of different entities have been registered during the construction, with the largest one occurring in 1974 due to flow liquefaction. When this slump occurred, a compacted cell 12.8 m high and about 36 m wide with a front slope of 1V:1H, was being placed on an approximately 9 m thick layer of loose sand recently deposited. The cell was placed in five lifts over the period from May 14 to August 22, 1974. During the construction of the first four lifts, no failure signals were observed, while the slump started near the completion of the last lift when the final compaction works were being carried out. The compacted cell did not liquefy and behaved as a rigid slab, while the beach sand below the cell liquefied and flowed out into the pond, generating a rapid failure. According to Plewes et al. (1989), the increased

construction rate and the considerable height of the compacted cell may have been the reasons for inducing static liquefaction.

The geometry of the model is shown in Figure 2, with the water table indicating the pond level on the upstream and falling within the dyke due to the downstream drainage system (Shuttle et al., 2021b). The bottom of the model is fully fixed, while the two lateral boundaries are normally fixed.

The finite element model has been discretised using a very fine mesh with 15-noded triangular elements, and with different degrees of local mesh refinement where significant changes in stresses and strains are expected during the analysis (i.e. in the loose beach sand below the compacted cell).

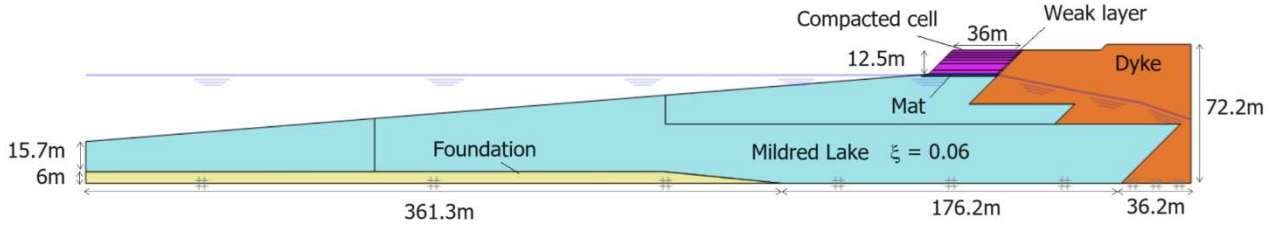

Figure 2. Model geometry in PLAXIS 2D.

The compacted dyke embankment, the compacted cell and the foundation layer have been modelled using drained Mohr-Coulomb model (Table 1).

Table 1. Parameters values for Mohr-Coulomb model.

γ_{unsat}	γ_{sat}	G	ν'	c'	φ'
18.6	19.6	33.3	0.2	5	48
kN/m^3	kN/m^3	MPa	-	kPa	°

For the foundation layer, an increased stiffness (G equal to 80 MPa) and strength (cohesion equal to 1 MPa) were assumed to simulate a rigid bedrock. The influence of a tension crack was considered by including a weak layer in between the compacted cell and the dyke, with a tension cut-off of 10 kPa and a friction angle of 5° (Shuttle et al., 2021b).

In this paper, the beach sand is assumed to consist entirely of loose material, modelled using CASM with a state parameter ξ of 0.06, while the mat at the bottom of the compacted cell consists of the same material but characterised by ξ equal to -0.1 (Shuttle et al., 2021b).

Since there were no investigations at that location at the time, Shuttle et al. (2021b) have selected the Mildred Lake data among test results available for tailings from existing mines in the area, determining the slope λ equal to 0.02826, the specific volume Γ of the CSL at a mean effective stress of 1 kPa equal to 1.89, and the stress ratio M equal to 1.29, i.e. a friction angle of about 32°. Additionally, the value of κ has been estimated equal to 0.004, based on the experimental data reported by Shuttle et al. (2021b).

The remaining model parameters characterising the shape of the yield surface and of the plastic potential should be calibrated based on laboratory tests. However, no tests are available for loose Mildred Lake material, which would be required for the calibration of CASM in problems involving flow liquefaction. For this reason, the calibration of the CASM parameters has been performed comparing the triaxial tests simulation results with those obtained with the NorSand (Jefferies, 1993) data set calibrated for the same application (Shuttle et al., 2021b). This results in a value of 20.4 for the spacing ratio r, 2 for n and 2.05 for m.

The initial stress state is generated assuming a coefficient of earth pressure at rest K_0 equal to 0.6, based on self-bored pressuremeter data at other tailings facilities, representing the case of normally consolidated tailings (Shuttle et al., 2021a, Shuttle et al., 2021b). The CASM parameters values are summarised in Table 2.

Table 2. CASM parameters values.

γ_{unsat}	γ_{sat}	λ	κ	ν'	φ
18.6	19.6	0.02826	0.004	0.2	32
kN/m^3	kN/m^3	-	-	-	°
n	r	m	Γ	ξ	K_0
2	20.4	2.05	1.89	0.06	0.6
-	-	-	-	-	-

The numerical analysis consists of six phases. In this study, we focus on reproducing the reported failure during the construction of the last tailings layer of which the increased of construction rate (Plewes et al., 1989) might be a contributing factor to flow liquefaction. Therefore, after the stress initialisation, the first four compacted layers are built in drained conditions, while the last one is built in undrained conditions. Considering the large strains expected in flow liquefaction problems, large deformation theory is taken into account in the construction phases through the Updated Lagrangian formulation (Bathe, 1982). Additionally, the arc-length control procedure

is adopted to improve the robustness of the analysis when dealing with failure in non-linear problems.

Three stress points have been selected to show the stress path evolution in the last phase, at the locations shown in Figure 3.

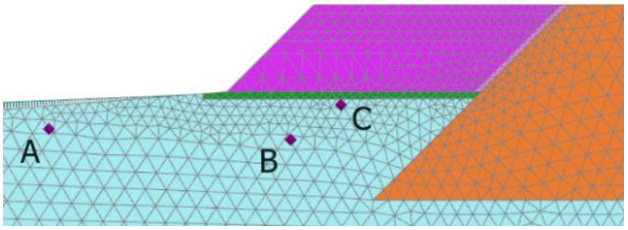

Figure 3. Selected stress points.

4 RESULTS

The first four construction stages are completed successfully while failure is detected during the activation of the top layer in undrained conditions.

During the last phase, prior to the occurrence of liquefaction, very small values of the deviatoric strain increment (in the order of 10^{-3}) are shown in Figure 4a. As expected, at the same step, the state parameter is positive in the loose beach sand, ranging from 0.04 to 0.06, approximately (Figure 4b).

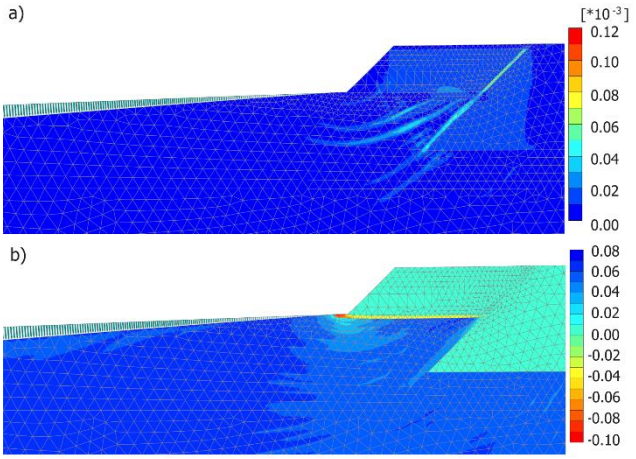

Figure 4. Contours prior to liquefaction occurrence: a) Deviatoric strain increment; b) State parameter.

In a subsequent step, shear bands develop (Figure 5a), along which the value of the state parameter approaches zero (Figure 5b), indicating that flow liquefaction has occurred.

Finally, at a later stage of liquefaction propagation, the deviatoric strain increment contours show multiple shear bands that extend to larger areas in the beach sand below the cell (Figure 6a). The state parameter is approximately zero in the same area (Figure 6b), showing that critical state has been reached. At the same step, the total displacement contours (Figure 6c) show that the compacted cell moves downwards, and that the depth of the collapsing mechanism extends to about 30 m below the cell.

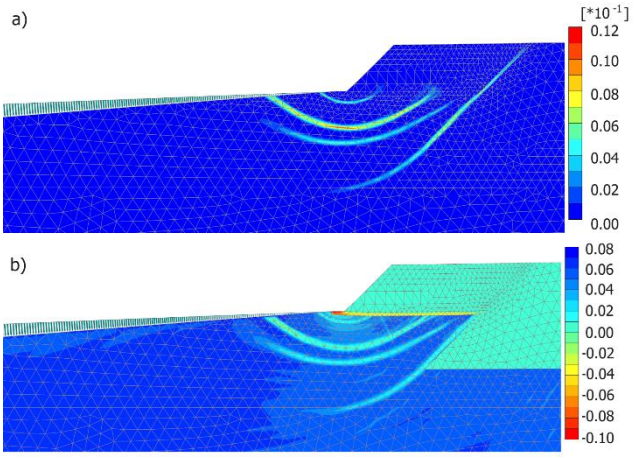

Figure 5. Contours at an early stage of liquefaction propagation: a) Deviatoric strain increment; b) State parameter.

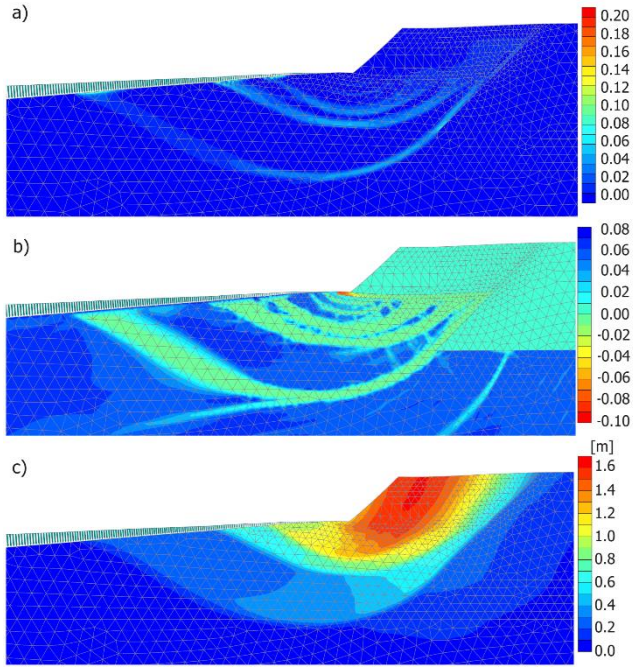

Figure 6. Contours at a later stage of liquefaction propagation: a) Deviatoric strain increment; b) State parameter; c) Total displacements.

A sharp decrease in terms of both deviatoric stress and mean pressure is observed along the shear bands, as shown by plotting the stress paths of the preselected stress points (Figure 7a). Starting from a relatively high value of p' and q, both stresses reduce, even to a value close to zero for point A, and reach the critical state line with a typical path indicating flow liquefaction. In the stress-strain plot (Figure 7b), undrained softening can be observed after a peak deviatoric stress is reached in each point.

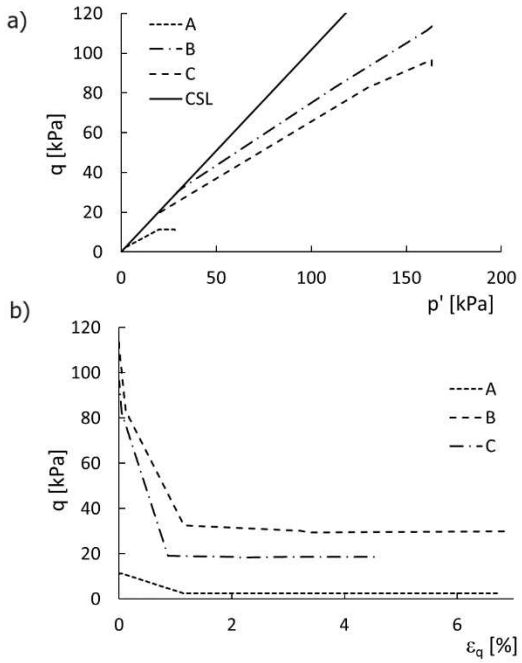

Figure 7. Results in preselected stress points: a) Stress paths; b) Stress-strain response.

5 CONCLUSION

This paper shows the capabilities of CASM to simulate undrained softening and reproduce the behaviour of soils susceptible to flow liquefaction. The model has been implemented as a user-defined soil model in PLAXIS and includes some improvements with respect to the original formulation, such as Lode's angle dependency, an alternative plastic potential equation and the possibility to account for creep effects.

In this paper, CASM has been calibrated based on available data and triaxial tests simulations on loose tailings. The Tar Island Dyke has been selected as a case study, where a major failure event caused by flow liquefaction of loose beach sand has been recorded in 1974. The results of the finite element analysis are consistent with the observations and show that CASM is capable of reproducing the behaviour of loose tailings in both drained and undrained conditions. In particular, the model is suitable for applications in which flow liquefaction may occur.

REFERENCES

Alonso, E. E., and Gens, A. (2006). Aznalcóllar dam failure. Part 3: Dynamics of the motion. *Géotechnique*, 56(3), pp. 203-210. https://doi.org/10.1680/geot.2006.56.3.203.

Arroyo, M., and Gens, A. (2021). Computational analyses of Dam I failure at the Corrego de Feijao mine in Brumadinho. Final report to VALE S.A.

Bathe, K.J. (1982). Finite element nonlinear analysis in solid and structural mechanics, In: *Finite element analysis in engineering analysis.* Prentice-Hall, New Jersey, United States.

Been, K., and Jefferies, M. (1985). A state parameter for sands. *Géotechnique*, 35(2), pp. 99-112. https://doi.org/10.1680/geot.1985.35.2.99.

Bentley Systems Inc. (2023). PLAXIS 2D (23.02). Available at: https://www.bentley.com/software/ plaxis-2d, accessed: 30/11/2023.

Jefferies, M. (1993). Nor-Sand: A simple critical state model for sand. *Géotechnique*, 43(1), pp. 91-103. https://doi.org/10.1680/geot.1993.43.1.91.

Mánica, M.A., Arroyo, M. and Gens, A. (2021). Effects of tailings viscosity on liquefaction triggering analyses. In: *Tailings and mine waste '21: proceedings of the twenty-fifth international conference on tailings and mine waste.* pp. 372-381. University of Alberta, Banff, Canada.

Mánica, M. A., Arroyo, M., Gens, A., and Monforte, L. (2022). Application of a critical state model to the Merriespruit tailings dam failure. *Proceedings of the Institution of Civil Engineers-Geotechnical Engineering*, 175(2), pp. 151-165. https://doi.org/10.1680/jgeen.21.00001.

Morgenstern, N. R., Vick, S. G., Viotti, C. B., and Watts, B. D. (2016). Report on the Immediate Causes of the Failure of the Fundão Dam. Fundão Tailings Dam Review Panel.

Plewes H.D., O'Neill H.D., McRoberts E.C., and Chan W.K. (1989). *Liquefaction considerations for Suncor Tailings Ponds.* Second Alberta Dam Safety Seminar, Edmonton, Alberta, Canada.

Rowe, P. W. (1962). The stress-dilatancy relation for static equilibrium of an assembly of particles in contact. *Proceedings of the Royal Society of London. Series A. Mathematical and Physical Sciences*, 269(1339), pp. 500-527. https://doi.org/10.1098/rspa.1962.0193.

Schofield, A. N., and Wroth, P. (1968). Critical state soil mechanics. Vol. 310. McGraw-Hill, London, United Kingdom.

Sheng, D., Sloan, S.W., and Yu, H.S. (2000). Aspects of finite element implementation of critical state models. *Computational mechanics*, 26, pp. 185-196. https://doi.org/10.1007/s004660000166.

Shuttle, D., Martens, S., and Jefferies, M. (2021a). Geostatic stress in oilsand tailings. *Proceedings of the Institution of Civil Engineers–Geotechnical Engineering.* https://doi.org/10.1680/jgeen.21.00114.

Shuttle, D., Marinelli, F., Brasile, S., and Jefferies, M. (2021b). Validation of computational liquefaction for tailings: Tar Island slump. *Geotechnical Research*, 9(1), pp. 32-55. https://doi.org/10.1680/jgere.21.00007

Yu, H.S. (1998). CASM: A unified state parameter model for clay and sand. *International journal for numerical and analytical methods in geomechanics,* 22(8), pp. 621-653.

INTERNATIONAL SOCIETY FOR SOIL MECHANICS AND GEOTECHNICAL ENGINEERING

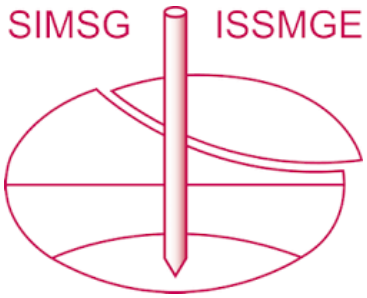

This paper was downloaded from the Online Library of the International Society for Soil Mechanics and Geotechnical Engineering (ISSMGE). The library is available here:

https://www.issmge.org/publications/online-library

This is an open-access database that archives thousands of papers published under the Auspices of the ISSMGE and maintained by the Innovation and Development Committee of ISSMGE.

The paper was published in the proceedings of the 18th European Conference on Soil Mechanics and Geotechnical Engineering and was edited by Nuno Guerra. The conference was held from August 26th to August 30th 2024 in Lisbon, Portugal.